Molecular Vision 2020; 26:291-298 <http://www.molvis.org/molvis/v26/291>
Received 29 October 2019 | Accepted 9 April 2020 | Published 11 April 2020

Clinical findings and *RS1* genotype in 90 Chinese families with X-linked retinoschisis

Chunjie Chen, Yue Xie, Tengyang Sun, Lu Tian, Ke Xu, Xiaohui Zhang, Yang Li

Beijing Institute of Ophthalmology, Beijing Tongren Eye Center, Beijing Tongren Hospital, Capital Medical University, Beijing Ophthalmology & Visual Sciences Key Lab. Beijing, China

Purpose: X-linked retinoschisis (XLRS) is an early-onset retinal degenerative disorder caused by mutations in the *RS1* gene. The objective of this study was to describe the clinical and genetic findings in 90 unrelated Chinese patients with XLRS.

Methods: All patients underwent clinical examination, including best-corrected visual acuity (BCVA), slit-lamp biomicroscopy, fundus examination, and spectral domain–optical coherence tomography (SD-OCT). A combination of molecular screening methods, including Sanger-DNA sequencing of *RS1* and targeted next-generation sequencing (TES), were used to detect mutations. In silico programs were used to analyze the pathogenicity of all the variants. Long-range PCR with subsequent DNA sequencing was employed to find the breakpoints of large deletions.

Results: The 90 probands (mean age 17.29±12.94 years; 3–52 years) showed a variety of clinical phenotypes, and their average best correct visual acuity was 0.81±0.48 (logarithm of the minimal angle of resolution, 0–3). Of the 175 eyes analyzed, 140 (80%) had macular retinoschisis, 84 (48%) had peripheral retinoschisis, 28 (16%) had macular atrophy, and five (3%) had a normal macular structure. We identified 68 mutations in this cohort of patients, including 15 novel mutations. Most mutations (65%) were missense; the remaining null mutations included nonsense, splicing effect, frameshift indel, and large genomic DNA deletions. The 62 patients with missense mutations seemed to have relatively milder visual defects than the 28 patients with null mutations.

Conclusions: Patients with *RS1* mutations present profound phenotypic variability and show no clear genotype–phenotype correlations. Patients with null mutations tend to have more severe XLRS-related visual defects.

X-linked retinoschisis (XLRS; OMIM 312700), an early-onset retinal degenerative disorder, is transmitted in an X-linked recessive pattern and almost exclusively affects males [1,2]. Patients with XLRS usually present with visual defects of various extents in their first decade of life and macular retinoschisis in a spoke-wheel pattern [1,2]. About 50% of these patients also have peripheral or mid-peripheral retinoschisis, mostly located in the inferotemporal quadrant [3]. The disease usually exhibits slow, minimal progression; the exceptions are secondary complications, such as retinal detachment and vitreous hemorrhage, which can lead to severe visual impairments [3,4]. ERGs used to be key diagnostic examinations for patients with XLRS, as these patients would typically display reduced b-wave amplitude with relative preservation of a-wave amplitude (b/a wave ratio below 1.0) when their dark-adapted retinas were stimulated with bright flashes of light [5].

XLRS is caused by mutations in the *RS1* (Gene ID: 6247; OMIM: 300839) gene in Xp22.1; this gene encodes a 224 amino acid protein, retinoschisin (RS) [6]. The RS protein consists of an N-terminal leader sequence, an Rs1 domain, a discoidin domain, and a C-terminal segment. RS is highly expressed in photoreceptor cells and within the inner portions of the retina [6,7]. The discoidin domain of RS is homologous to similar proteins involved in cell adhesion, suggesting that RS might play an important part in maintaining the structural integrity of the retina [7,8]. So far, over 200 mutations of the *RS1* gene have been reported, and most are missense mutations identified in exons 4–6, which encode the discoidin domain [5,6,9–20]. Other kinds of mutations, including nonsense, splicing effect, frameshift small insert or deletions, and large deletions, have also been identified [9–20].

Many previous studies have compared *RS1* genotypes and XRLS phenotypes, but most found no relationship between *RS1* mutations and clinical severity [10–15]. However, some studies have described severe visual impairments in patients with mutations in exons 1–3 or with large deletions of exon 1 [16,17]. One study indicated that patients with null mutations consistently showed electronegative bright-flash ERG results, delayed flicker responses, and abnormal-pattern ERG results, while patients with missense mutations presented a wider range of ERG abnormalities [14]. The purpose of this study was to describe the genetic and clinical features of 90

Correspondence to: Yang Li, Beijing Institute of Ophthalmology, Beijing Tongren Hospital, Hougou Lane 17, Chong Nei Street, Beijing, 100730, China. Phone: 8610-58265915; FAX: 8610-65288561 or 65130796; email: yanglibio@aliyun.com

unrelated Chinese patients with XLRS and to report any genotype–phenotype correlations.

METHODS

This was a retrospective, observational cross-sectional study. The study procedures were performed in accordance with the institutional instructions of the Beijing Tongren Hospital Joint Committee on Clinical Investigation and adhered to the tenets of the Helsinki Declaration. Informed consent was obtained from all patients after a full explanation of the procedures. Most patients were initially diagnosed with XLRS based on their clinical evaluations and family histories. Their diseases were further confirmed by identifying disease-causing mutations of the *RS1* gene in the Genetics Laboratory of the Beijing Institute of Ophthalmology, Beijing Tongren Ophthalmic Center from 2010–2018. We recruited a total of 90 unrelated male patients from Beijing Tongren Hospital; of these, 40 probands had family histories. The patients included 27 probands previously reported [18,19]. All patients underwent standard ophthalmological examination consisting of best-corrected visual acuity (BCVA), slip-lamp biomicroscopy, and fundus examination. Eighty-three patients also had optical coherence tomography (OCT) examinations (Heidelberg OCT SPECTRALIS, Heidelberg, Germany or Ivue-100, Optovue Inc., Fremont, CA). Thirteen patients underwent fundus autofluorescence (FAF; Heidelberg OCT SPECTRALIS, Heidelberg, Germany), and 12 probands had full-field ERG examinations.

Peripheral blood samples for genetic analysis were collected from all the probands and their available relatives. Genomic DNA was then extracted using a genomic DNA extraction and purification kit (Vigorous Whole Blood Genomic DNA Extraction Kit; Vigorous, Beijing, China) following the manufacturer's protocol.

PCR-based sequencing of the RS1 gene: All exons and flanking splicing sites of the *RS1* gene were amplified by PCR in 87 probands. The PCR amplifications were performed using standard reaction mixtures, and the purified amplified fragments were sequenced using an ABI Prism 373A DNA sequencer (Applied Biosystems, Foster City, CA), as previously described [18]. A published cDNA sequence for *RS1* (GenBank NM_000330) was compared with the sequencing results.

Targeted exome sequencing: We used a targeted exome sequencing (TES) panel developed previously to conduct TES on three patients initially diagnosed with retinitis pigmentosa or inherited macular dystrophy [21]. The capture panel consisted of 188 known inherited retinal degeneration genes. The Illumina library preparation and capture experiments were performed as previously reported [21]. Briefly, genomic DNA (1–3 μg) was fragmented into approximately 300–450 base pairs by endonuclease digestion and used to capture the targeted genomic sequences. The enrichment libraries were sequenced as 100-bp paired-end reads on an Illumina NextSeq 500 (Illumina, Inc., San Diego, CA) according to the manufacturer's protocol. The raw sequencing data processing, calling, and analysis were performed as previously described [21]. First, the Illumina sequencing adapters and low-quality reads were removed using fastq_mcf software. Then, the duplicated reads were removed using Picard tools, and the high-quality reads were aligned with the reference human genome (hg19) using the Burrows-Wheeler Aligner. Finally, the single nucleotide polymorphisms (SNPs) and insertions or deletions (InDels) were called using the Genomic Analysis Toolkit Haplotype Caller.

Bioinformatics analysis: Two databases, the HGMD database and the LOVD database, were used to search for reported pathogenic mutations. The pathogenicity of variants was predicted by three in silico programs: PolyPhen2, Mutation Taster, and SIFT. Co-segregations were analyzed if DNA from family members was available.

Statistical analysis: All statistical analyses were performed using IBM SPSS statistical software (v25.0; SPSS Inc., Chicago, IL). BCVA was converted to the logarithm of the minimal angle of resolution (logMAR) for statistical analysis. Values of 0, 1.0, 2.0, and 3.0 in logMAR, respectively, corresponded to 1.0, 0.1, counting fingers, and hand movement in Snellen visual acuity [22]. Light or no light perception was excluded [22]. The Pearson correlation coefficient and linear regression analysis were used to evaluate the association of BCVA and age in all patients, in group A patients who carried the missense mutation, and in group B patients who harbored null or run-on mutations. Run-on mutation indicated a base change, cause the normal stop codon becoming an amino acid codon, so translation is predicted to continue into the 3'UTR. Differences between the two genotype groups were analyzed using the Mann–Whitney U Test for age at visit and BCVA. The chi-square test was used to analyze the differences in clinical features between groups A and B. When fourfold table data of sample size $n<40$ or at least one of the four quadrants had a frequency $T<1$, the Fisher probabilities were used in the 2×2 table method. A p value less than 0.05 was considered statistically significant.

RESULTS

RS1 mutations: We identified 68 distinct hemizygous mutations of the *RS1* gene in the 90 probands (Appendix 1). Of these mutations, 15 were newly detected in the current

study. The mutations included 44 missense mutations, eight nonsense mutations, eight splicing effects, four frameshift small insertion/deletions (indel), two large deletions, and two run-on mutations (Figure 1A). The most frequently encountered mutations were p.E72K and p.R213W, each found in four probands (4.4%, 4/90), followed by the mutations p.R102Q, p.R141H, p.W163X, p.R200C, and p.R209H, each identified in three probands (3.3%, 3/90). The remaining mutations were detected either twice (seven mutations) or only once (54 mutations). The 15 novel mutations included ten missense, two splicing effect, two frameshift indel, and one nonsense mutation. None of these novel mutations were found in any public databases or in our 100 normal controls. The ten missense mutations were predicted to be disease-causing or probably damaging by at least two in silico analysis programs. We used long-range PCR to define breakpoints in the two large deletions: The first was a 15.4 kb deletion that covered part of the 5′UTR and exon 1 and most of intron 1, and the second was a 6.3 kb deletion that encompassed part of intron 3 and exons 4–6 and part of the 3′UTR (Figure 1B).

Clinical profiles: The 90 unrelated patients in the current study all experienced different extents of defects in visual acuity; six also complained of night blindness, and three had hearing-loss symptoms. These patients had an average age at diagnosis of 17.29±12.94 years (3–52 years), and their mean BCVA was 0.81±0.48 (logMAR from 3–0). Most patients showed fundus appearances typical of RS (Figure 2); however, some presented atypical fundus changes (Figure 3). Of the 90 patients, eight experienced vitreous hemorrhage (VH), six had retinal detachment (RD), and one suffered both VH and RD according to their medical records and fundus photos or ocular ultrasound scans. The average age of onset for the nine patients diagnosed with VH was 5.13±2.75 years (1.5–35 years), and the mean age of onset for the seven patients presenting RD was 5.43±2.99 years (1.5–9.5 years). Overall, 76 patients showed almost symmetric lesions in both eyes, nine presented asymmetric retinoschisis or macular atrophy in their eyes, and five had only one eye analyzed (the other eyes excluded because of the presence of dense cataracts, keratoleukoma, or VH). Appendix 2 summarizes the detailed clinical features of each patient. Fundus examinations revealed that 140 (80%) of 175 eyes had macular retinoschisis, 84 (48%) had peripheral retinoschisis, 28 (16%) had macular atrophy, and five (3%) presented normal macular structures. In total, 130 of the 140 eyes with macular retinoschisis and 25 of the 28 eyes with macular atrophy were evaluated using a combination of both clinical and OCT examinations. Of the 175 eyes, 32 (18%) showed RPE pigment migration, 20 (11%) showed vitreous veils, 18 (10%) presented vascular sheathing, and 12 (7%) had white dots. Of the total 180 eyes, eight (4.4%) had RD and nine (5.0%) experienced VH.

Genotype–phenotype correlations: Genetic analysis revealed 62 patients (group A) harboring missense mutations and 28 (group B) carrying null or run-on mutations. In this current cohort, the BCVA of all patients was statistically correlated with patient age (R = 0.107, p = 0.047); however, the visual impairments tended to be more severe in group B than in group A (Figure 4A). RPE pigment migration was more frequently observed in the group B patients (C = 0.16, p = 0.031; Figure 4B). No significant difference was observed in the percentages of patients showing asymmetric fundus appearances; these ratios were 14.5% (9/62) for group A and 17.9% (5/28) for group B.

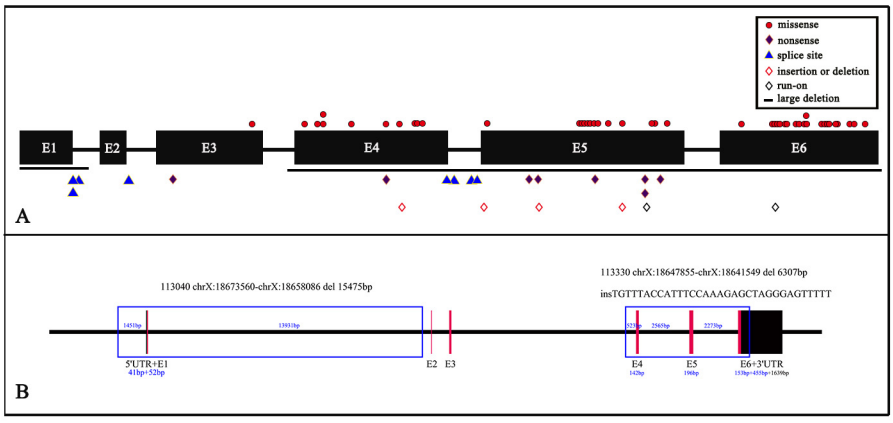

Figure 1. The distribution of 68 distinct mutations of *RS1* detected in our study and the breakpoints in two large deletions. **A**: The distribution of 68 mutations on exons of *RS1*. **B**: Lengths and positions of the two gross deletions of *RS1* (in box with blue border). E indicates exon. Red squares indicate exons in coding regions. Black squares indicate exons in non-coding regions, and thick black lines indicate introns and upstream or downstream non-coding regions. The blue numbers indicate lengths of deletions in each corresponding region.

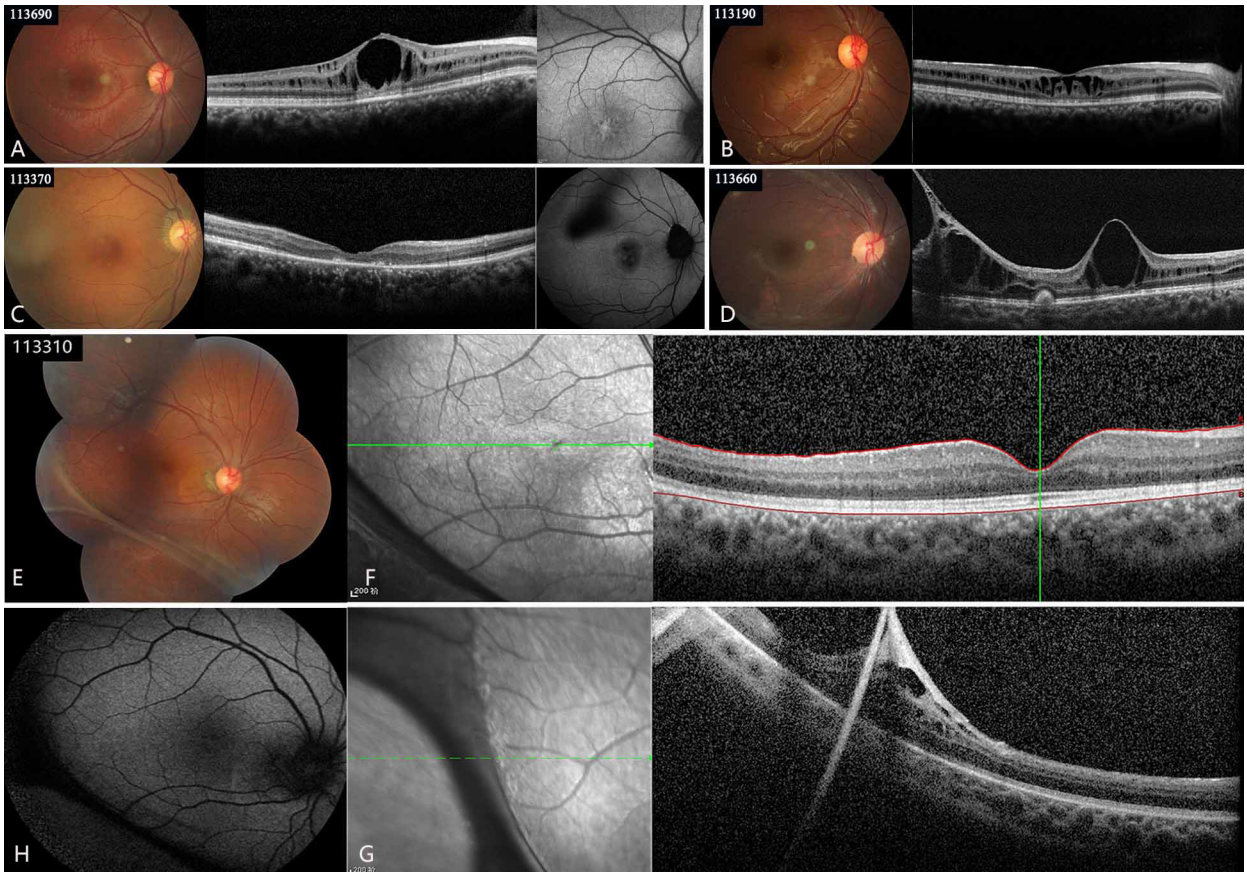

Figure 2. Colored fundus (CF) photographs, optical coherence tomography (OCT) scans, and fundus autofluorescence (FAF) of five patients with RS displaying typical macular and peripheral retinoschisis or macular atrophy. **A**: CF photographs, OCT scans, and FAF of patient 113690 showing macular retinoschisis and a spoke-wheel pattern of hyperfluorescence. **B**: CF photograph and OCT scan of patient 113190 displaying macular retinoschisis. **C**: CF photograph, OCT scan, and FAF of patient 113370 displaying macular atrophy and hypofluorescence in the macular region. **D**: CF photograph and OCT scan of patient 113660 presenting both macular and peripheral retinoschisis. **E**–**H**: CF photograph and OCT scan of patient 113310 showing normal macular structure (**E** and **F**) and peripheral retinoschisis (**E** and **G**). **H**: FAF of patient 113310 presenting almost-normal fluorescent pattern in the macular region and a hypofluorescent region corresponding to the peripheral retinoschisis.

DISCUSSION

The current study describes the genetic and clinical characteristics of 90 unrelated patients with molecularly confirmed XLRS. It represents one of the largest Chinese cohorts to date to undergo clinical and genetic analysis. Our results provide an outline of the prevalence of macular retinoschisis or atrophy and peripheral retinoschisis in a large cohort of patients with RS.

In this cohort of patients, we identified almost all types of mutations of the *RS1* gene. Most mutations were missense (65%, 44/68), a finding consistent with previous observations [9–20]. Except the mutation p.C59Y, the remaining 43 missense mutations were exclusively located in exons 4–6, which encode the discoidin domain of the *RS1* protein. We revealed two large genomic deletions in this study. The exon 1 deletion has been reported several times before and is frequently found in Danish patients [9,16,17]; however, only few of these previous studies defined the breakpoints at the genomic region [17]. The c.(−35)-1451_c.52+13931del15475 deletion identified in patient 113030 removed a core proximal promoter and a second *CRX*-bound region in intron 1 of *RS1* with multiple *CRX* sites; therefore, it likely modulates basal promoter activity [23–25]. It might cause a null allele with no XLRS protein produced. The c.167–532_c.580+2094del6307 detected in patient 113330 removed a genomic region spanning exons 4–6, which might cause abnormal splicing.

The patients in our cohort showed profound phenotypic variability, and we did not find any clear genotype or phenotype correlation. However, we did observe that the BCVA of all patients decreased with aging, which seemed more

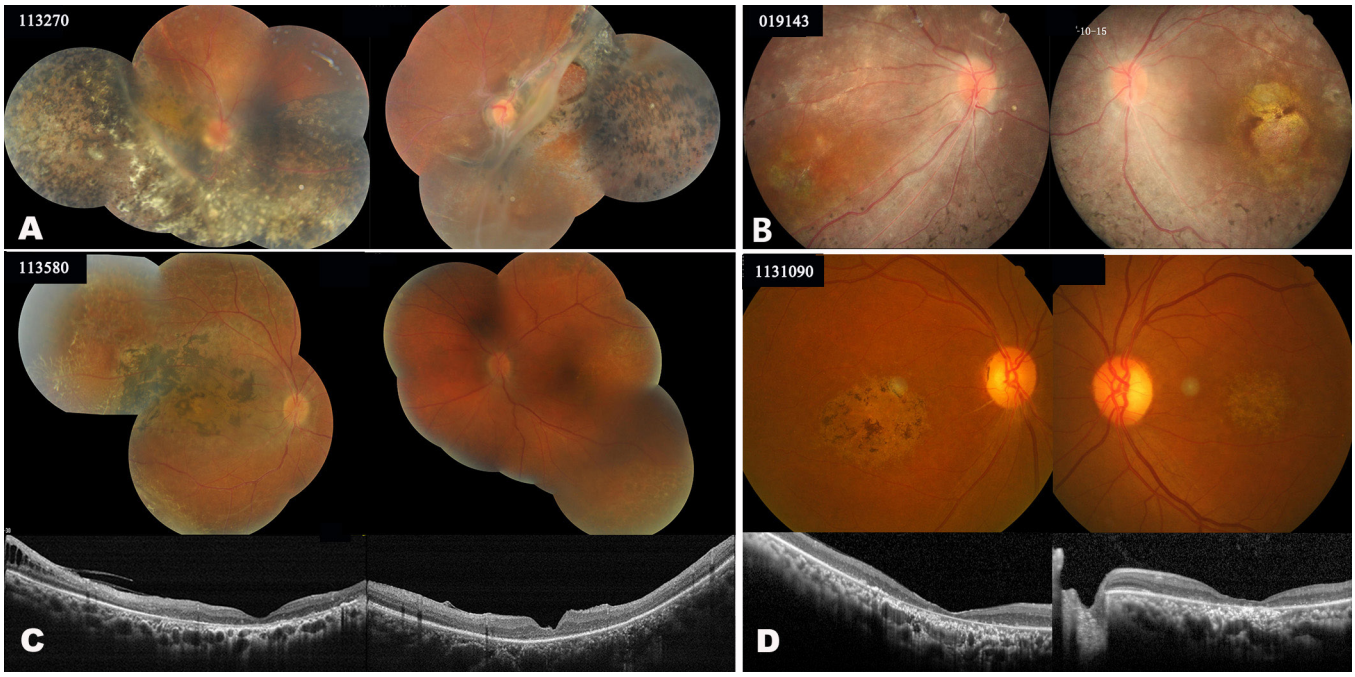

Figure 3. Colored fundus (CF) photographs and optical coherence tomography (OCT) scans of four patients with X-linked retinoschisis displaying atypical fundus appearances. **A**: CF photographs of patient 113270 showing bilateral peripheral retinoschisis involving the macula and severe retinal pigment degeneration with pigmentation, sheathed retinal vessels, and white dots at the temporal retina. **B**: CF photographs of patient 019143 presenting bilateral macular atrophy and retinal pigment degeneration with bone spicules and arteriole narrowing in the peripheral retina. **C**: CF photographs of patient 113580 showing macular atrophy with pigmentation, white spiculations in the peripheral retina of the right eye, and pigmentation in the peripheral retina of the both eyes and OCT scans presenting bilateral macular atrophy and peripheral retinoschisis in the right eye. **D**: CF photographs and OCT scans of patient 1131090 displaying symmetric macular atrophy with pigmentation.

evident in group B. One early study that included 86 patients with XLRS from the U.K. also found a decrease in visual acuity with increasing age; however, no correlation was noted between the severity of the disease and the mutation type [10]. Another genotype–phenotype correlation study revealed worse visual acuity in patients with null mutations than in those with missense mutations [14]. A recent prospective study that included 56 patients found almost-stable BCVA in patients during the 18-month follow-up period [26], further indicating that XLRS progression is slow.

We observed macular schisis, macular atrophy, and normal macular appearance in 81%, 16%, and 3% of the eyes in our cohort, respectively. The prevalence of macular schisis and atrophy was similar to that observed in Taiwanese patients [27]. We did not observe any significant difference between groups A and B in terms of the prevalence of macular schisis, which is consistent with the results of Vincent et al. [15]. As expected, patients with macular atrophy were usually older than the patients with macular schisis. This finding agrees with the natural history of XLRS, as macular schisis is usually followed by macular atrophy and schisis resolution [4]. Previous studies have observed that patients with normal macular structures usually carry missense mutations [14,15]; however, one of three patients with normal macular structures in our cohort had a splicing mutation. Four patients in the current cohort carried mutation p.E72K, one of the most common *RS1* mutations [9]. All four patients only presented with macular retinoschisis, which differed from the observations of three patients in an English cohort who all had vitreous veils [15]. In contrast to previous observations, patient 113,030, who had a large deletion that included exon 1, did not present a severe phenotype [16,17].

The prevalence of peripheral retinoschisis in this cohort was 48%, which was higher than the prevalence reported previously in Chinese patients (38% or 43%) [27,28] and English patients (33%) [15]. We did not observe any significant difference in the prevalence of peripheral retinoschisis between groups A and B; however, the incidence of peripheral pigmentary disturbances was significantly higher in group B. The rates of other peripheral findings, such as RPE pigment migration, vitreous veils, white dots, and vascular sheathing, were similar to those reported in English patients [15]. The

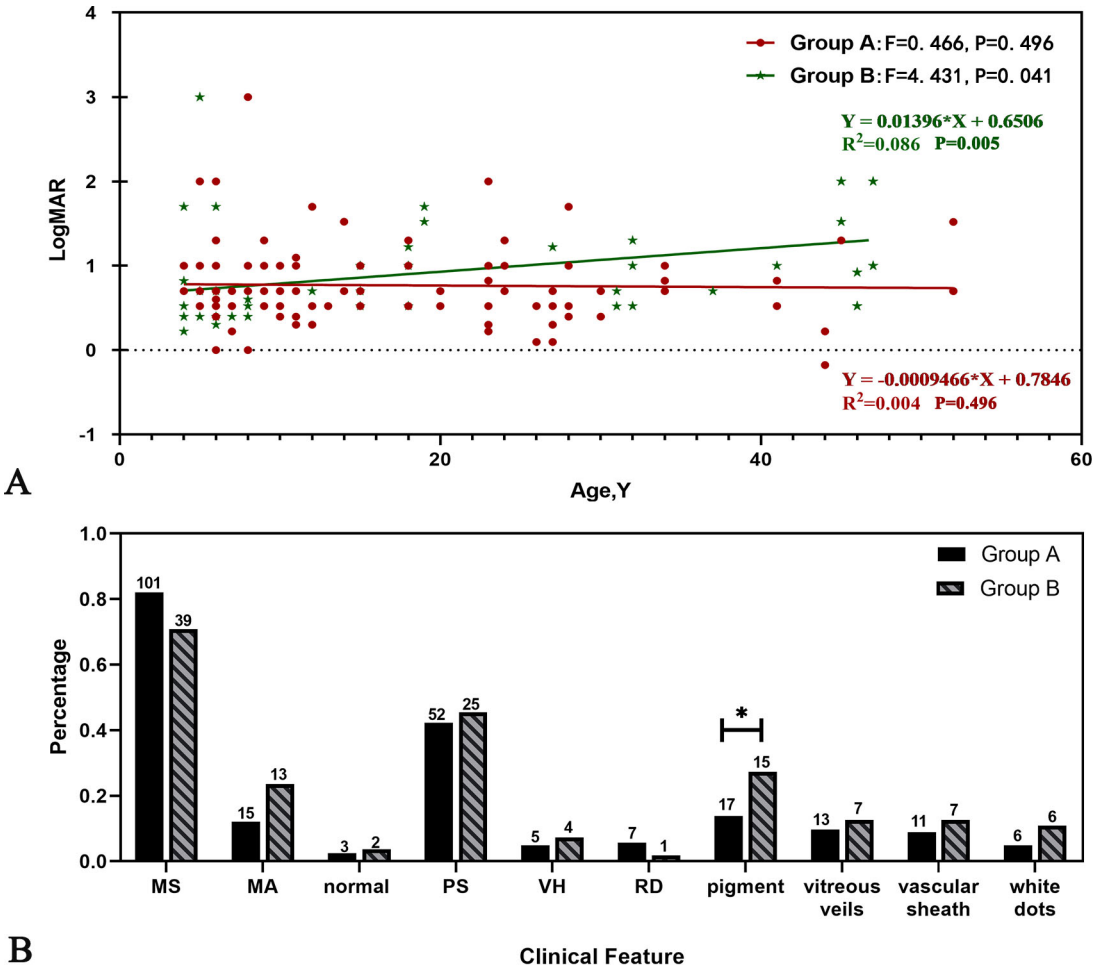

Figure 4. Comparison of the age, visual acuity, and clinical characteristics of groups A and B. **A**: Scatter plot and regression line of visual acuity with age in group A (red filled circles) and group B (solid green pentagrams). **B**: Bar chart of the clinical characteristics of the patients in groups A and B. Asterisks mark statistically significant differences ($p<0.05$). The numbers on the top of each bar indicate numbers of eyes with different clinical features.

rates of RD and VH were lower than the rates reported in an earlier study [3,4] but were similar to those found in an English cohort [15].

One limitation of this study was that only 12 patients underwent ERG examination. Therefore, we could not compare disease severity with the type of ERG abnormality. Other limitations were the retrospective design and the lack of longitudinal observation.

In conclusion, patients with *RS1* mutations present profound phenotypic variability and show no clear genotype–phenotype correlations, and patients with null mutations tend to have more severe XLRS-related visual defects.

APPENDIX 1. PRESUMED PATHOGENIC RS1 VARIANTS IDENTIFIED IN THIS STUDY AND ANALYSIS OF THE VARIANTS BY PREDICTIVE PROGRAMS.

To access the data, click or select the words "Appendix 1."

APPENDIX 2. THE CLINICAL FEATURES AND THE MUTATION SCREENING RESULTS OF THE PATIENTS IN THIS STUDY.

To access the data, click or select the words "Appendix 2."

ACKNOWLEDGMENTS

This work was supported by the National Key R&D Program of China, 2016YFC0905200. The funding organization had no role in the design or conduct of this research.

REFERENCES

1. Molday RS, Kellnerb U, Weber BHF. X-linked juvenile retinoschisis: Clinical diagnosis, genetic analysis, and molecular mechanisms. Prog Retin Eye Res 2012; 31:195-212. [PMID: 22245536].
2. Kim DY, Mukai S. X-linked Juvenile Retinoschisis (XLRS): A review of genotype-phenotype relationships. Semin Ophthalmol 2013; 28:392-6. [PMID: 24138048].
3. George ND, Yates JR, Moore AT. Clinical features in affected males with X-linked retinoschisis. Arch Ophthalmol 1996; 114:274-80. [PMID: 8600886].
4. Roesch MT, Ewing CC, Gibson AE, Weber BH. The natural history of X-linked retinoschisis. Can J Ophthalmol 1998; 33:149-58. [PMID: 9606571].
5. Renner AB, Kellner U, Fiebig B, Cropp E, Foerster MH, Weber BH. ERG variability in X-linked congenital retinoschisis patients with mutations in the RS1 gene and the diagnostic importance of fundus autofluorescence and OCT. Doc Ophthalmol 2008; 116:97-109. [PMID: 17987333].
6. Sauer CG, Gehrig A, Warneke-Wittstock R, Marquardt A, Ewing CC, Gibson A, Lorenz B, Jurklies B, Weber BH. Positional cloning of the gene associated with X-linked juvenile retinoschisis. Nat Genet 1997; 17:164-70. [PMID: 9326935].
7. Molday LL, Hicks D, Sauer CG, Weber BH, Molday RS. Expression of X- linked retinoschisis protein RS1 in photoreceptor and bipolar cells. Invest Ophthalmol Vis Sci 2001; 42:816-25. [PMID: 11222545].
8. Molday RS. Focus on molecules: retinoschisin (RS1). Exp Eye Res 2007; 84:227-8. [PMID: 16600216].
9. . The Retinoschisis Consortium. Functional implications of the spectrum of mutations found in 234 cases with X-linked juvenile retinoschisis (XLRS). Hum Mol Genet 1998; 7:1185-92. [PMID: 9618178].
10. Pimenides D, George ND, Yates JR, Bradshaw K, Roberts SA, Moore AT, Trump D. X-linked retinoschisis: clinical phenotype and RS1 genotype in 86 UK patients. J Med Genet 2005; 42:e35-[PMID: 15937075].
11. Hewitt AW, FitzGerald LM, Scotter LW, Mulhall LE, McKay JD, Mackey DA. Genotypic and phenotypic spectrum of X-linked retinoschisis in Australia. Clin Experiment Ophthalmol 2005; 33:233-9. [PMID: 15932525].
12. Riveiro-Alvarez R, Trujillo-Tiebas MJ, Gimenez-Pardo A, Garcia-Hoyos M, Lopez-Martinez MA, Aguirre-Lamban J, Garcia-Sandoval B, Vazquez-Fernandez del Pozo S, Cantalapiedra D, Avila-Fernandez A, Baiget M, Ramos C, Ayuso C. Correlation of genetic and clinical findings in Spanish patients with X-linked juvenile retinoschisis. Invest Ophthalmol Vis Sci 2009; 50:4342-50. [PMID: 19324861].
13. Bowles K, Cukras C, Turriff A, Sergeev Y, Vitale S, Bush RA, Sieving PA. X–Linked Retinoschisis: RS1 mutation severity and age affect the ERG phenotype in a cohort of 68 affected male subjects. Invest Ophthalmol Vis Sci 2011; 52:9250-6. [PMID: 22039241].
14. Vincent A, Robson AG, Neveu MM, Wright GA, Moore AT, Webster AR, Holder GE. A phenotype-genotype correlation study of X-linked retinoschisis. Ophthalmology 2013; 120:1454-64. [PMID: 23453514].
15. Fahim AT, Ali N, Blachley T, Michaelides M. Peripheral fundus findings in X-linked retinoschisis. Br J Ophthalmol 2017; 101:1555-9. [PMID: 28348004].
16. Chan WM, Choy KW, Wang J, Lam DS, Yip WW, Fu W, Pang CP. Two cases of X-linked juvenile retinoschisis with different optical coherence tomography findings and RS1 gene mutations. Clin Experiment Ophthalmol 2004; 32:429-32. [PMID: 15281981].
17. D'Souza L, Cukras C, Antolik C, Craig C, Lee J, He H, Li S, Smaoui N, Hejtmancik JF, Sieving PA, Wang X. Characterization of novel RS1 exonic deletions in juvenile X-linked retinoschisis. Mol Vis 2013; 19:2209-16. [PMID: 24227916].
18. Chen J, Xu K, Zhang X, Pan Z, Dong B, Li Y. Novel mutations of the RS1 gene in a cohort of Chinese families with X-linked retinoschisis. Mol Vis 2014; 20:132-9. [PMID: 24505212].
19. Jiang F, Chen J, Xu K, Zhang X, Li Y. Characteristics of RS1 genotype in Chinese patients with X-linked retinoschisis Ophthalmology in China 2015; 24:90-5. J.
20. Li X, Ma X, Tao Y. Clinical features of X linked juvenile retinoschisis in Chinese families associated with novel mutations in the RS1 gene. Mol Vis 2007; 13:804-12. [PMID: 17615541].
21. Sun T, Xu K, Ren Y, Xie Y, Zhang X, Tian L, Li Y. Comprehensive molecular screening in Chinese Usher Syndrome patients. Invest Ophthalmol Vis Sci 2018; 59:1229-37. [PMID: 29625443].
22. Holladay JT. Proper method for calculating average visual acuity. J Refract Surg 1997; 13:388-91. [PMID: 9268940].
23. Cheng H, Khanna H, Oh EC, Hicks D, Mitton KP, Swaroop A. Photoreceptor-specific nuclear receptor NR2E3 functions as a transcriptional activator in rod photoreceptors. Hum Mol Genet 2004; 13:1563-75. [PMID: 15190009].
24. Haider NB, Naggert JK, Nishina PM. Excess cone cell proliferation due to lack of a functional NR2E3 causes retinal dysplasia and degeneration in rd7/rd7 mice. Hum Mol Genet 2001; 10:1619-26. [PMID: 11487564].
25. Mears AJ, Kondo M, Swain PK, Takada Y, Bush RA, Saunders TL, Sieving PA, Swaroop A. Nrl is required for rod photoreceptor development. Nat Genet 2001; 29:447-52. [PMID: 11694879].
26. Pennesi ME, Birch DG, Jayasundera KT, Parker M, Tan O, Gurses-Ozden R, Reichley C, Beasley KN, Yang P, Weleber RG, Bennett LD, Heckenlively JR, Kothapalli K, Chulay JD. For The Xlrs-Study Group. Prospective evaluation of patients with X-linked retinoschisis during 18 months. Invest Ophthalmol Vis Sci 2018; 59:5941-56. [PMID: 30551202].
27. Wang NK, Liu L, Chen HM, Tsai S, Chang TC, Tsai TH, Yang CM, Chao AN, Chen KJ, Kao LY, Yeung L, Yeh LK, Hwang YS, Wu WC, Lai CC. Clinical presentations of X-linked

retinoschisis in Taiwanese patients confirmed with genetic sequencing. Mol Vis 2015; 21:487-501. .

28. Hu QR, Huang LZ, Chen XL, Xia HK, Li TQ, Li XX. Genetic analysis and clinical features of X-linked retinoschisis in Chinese patients. Sci Rep 2017; 7:44060-[PMID: 28272453].

Articles are provided courtesy of Emory University and the Zhongshan Ophthalmic Center, Sun Yat-sen University, P.R. China. The print version of this article was created on 11 April 2020. This reflects all typographical corrections and errata to the article through that date. Details of any changes may be found in the online version of the article.